Applied Thermal Engineering 302 (2026) 131972

Contents lists available at ScienceDirect

Applied Thermal Engineering

journal homepage: www.elsevier.com/locate/apthermeng

Research Paper

Polydimethylsiloxane based transparent and reflective materials for passive daytime radiative cooling

Zesen Su [a], Prit Patel [a], Haiying Cheng [a], Bryce S. Richards [a,b], Gan Huang [a,*]

[a] Institute of Microstructure Technology, Karlsruhe Institute of Technology, Hermann-von-Helmholtz-Platz 1, 76344 Eggenstein-Leopoldshafen, Germany
[b] Light Technology Institute, Karlsruhe Institute of Technology, Engesserstrasse 13, 76131 Karlsruhe, Germany

ARTICLE INFO

Keywords:
Radiative cooling
Polymer
Solar reflector

ABSTRACT

Passive daytime radiative cooling (PDRC) dissipates heat by emitting infrared radiation through the atmospheric transparency window (8–13 μm), enabling sub-ambient temperatures under direct sunlight without energy input. Polydimethylsiloxane (PDMS) is widely used in PDRC because it combines high emissivity in the 8–13 μm range with high transmittance (low absorption) in the solar spectrum (0.3–2.5 μm), while also being easy to fabricate. This study presents a systematic investigation of flat PDMS-based PDRC materials with thicknesses from around 1 μm to around 1000 μm deposited on either highly-transparent fused silica substrates or highly-reflective commercial sunlight reflector substrates. These configurations target applications such as cooling for transparent roofs and outdoor electronic enclosures. For a 58-μm-thick PDMS layer on silica, the sample shows a solar spectrum transmittance of 92.8%, absorption of 1.1%, and an emissivity of 94.4% in the 8–13 μm range, resulting in a net cooling power of 78.5 W/m^2. For this transparent configuration, the cooling power remains nearly unchanged for PDMS thicknesses from 1.7 μm to 121 μm, indicating a broad thickness tolerance for practical fabrication. For the PDMS-coated sunlight reflector sample with 60-μm-thick PDMS thickness, the absorption reaches 6.2%, which reduces the net cooling power to only 17.5 W/m^2. For this reflective configuration, an optimal PDMS thickness of around 60 μm is identified, but the cooling performance is strongly limited by the increased solar absorption of the reflector-based structure. This work highlights the potential of PDMS-based transparent and reflective materials for simple and scalable PDRC systems, while clarifying the influence of thickness and substrate choice on their cooling performance.

1. Introduction

The demand for sustainable cooling technologies continues to rise due to increasing global temperatures and the growing energy consumption associated with active cooling. Passive daytime radiative cooling (PDRC) has emerged as a promising strategy to reduce cooling loads with no additional electricity or thermal energy consumption [1–3]. PDRC relies on releasing heat from a surface into the cold outer space at around 3 K [4]. Any object above absolute zero emits thermal radiation, and the effectiveness to act as a PDRC depends on transferring this thermal radiation through the atmosphere while, at the same time, minimizing solar absorption. Although the atmosphere is highly absorptive at most infrared wavelengths, it exhibits a relative transparency window between 8 and 13 μm that enables thermal radiation to escape. PDRC materials require high emissivity within this window and low absorption in the solar spectrum (0.3–2.5 μm) to achieve sub-ambient cooling under sunlight.

Two general categories of PDRC materials exist [5–7]. Broadband emitters exhibit high emissivity across a wide mid-infrared range (5–25 μm), covering the atmospheric window. Selective emitters exhibit high emissivity primarily within the 8–13 μm window and low emissivity elsewhere. Both approaches enable sub-ambient cooling. Broadband materials tend to generate higher cooling power near ambient temperatures, while selective emitters can reach lower equilibrium temperatures due to reduced absorption of background thermal radiation. Several material developments mark milestones in the evolution of PDRC technology [5,7–10]. Early high-performance devices used multilayer hafnium dioxide and silicon dioxide nanophotonic stacks backed by silver reflectors [11] Scalable alternatives followed, including polymer composites with silica microspheres, porous polymer membranes with strong solar backscattering [12] and, more recently, porous ceramic structures with enhanced outdoor stability [13] Alongside these

* Corresponding author.
E-mail address: gan.huang@kit.edu (G. Huang).

https://doi.org/10.1016/j.applthermaleng.2026.131972
Received 16 April 2026; Received in revised form 5 June 2026; Accepted 13 June 2026
Available online 15 June 2026

rapid advances, there has also been growing interest in simple and low cost PDRC materials. Among these, polydimethylsiloxane (PDMS) [14–16] has received significant attention. PDMS exhibits strong intrinsic vibrational absorption within the 8–13 μm atmospheric window, enabling efficient thermal emission, while remaining highly transparent to solar radiation. It is flexible, chemically stable, resistant to ultraviolet (UV) radiation, and compatible with scalable fabrication methods such as solution casting, spin coating, blade coating, and molding. Even without additional micro- or nano-structuring, flat PDMS films have demonstrated effective daytime cooling [15,17,18]. For example, a 100 μm PDMS film on a silver reflector (120 nm-thick silver coating) can achieve approximately 8 °C sub-ambient cooling [18]. Herrmann et al. systematically investigated the PDRC performance of PDMS films deposited on silver reflectors with a 100 nm-thick silver coating, using PDMS thicknesses ranging from 712 nm to 2.35 mm[19]. Their results showed that the cooling performance reached a maximum at a PDMS thickness of approximately 88 μm, demonstrating that the optical thickness of the PDMS layer plays a critical role in balancing solar absorption and mid-infrared emission. This finding highlights the necessity of optimizing the PDMS layer thickness rather than simply increasing it to enhance emissivity. Zhou et al. reported a configuration in which a 150-μm-thick PDMS film was coated on a pure aluminium foil substrate [15]. Although aluminium foil offers a lower cost compared to silver coated reflectors, its higher solar absorption reduces the achievable daytime cooling performance. Therefore, solar shading was recommended in that work to suppress direct solar heating and improve the net cooling effect.

Despite these advantages, the performance of PDMS-based layers strongly depends on the choice of substrate. Previous studies have successfully demonstrated that metallic reflectors, such as sputtered silver/aluminium reflectors, can provide high solar reflectance and support efficient radiative cooling. However, the performance of PDMS-based PDRC layers on several practically-relevant commercial substrates remains insufficiently understood. For example, commercial sunlight reflectors are readily available and can be directly used as reflective substrates, while offering a balance among cost, durability, large-area scalability, and high solar reflectance. These attributes make them attractive candidates for large-scale and rapid deployment of reflective PDRC systems; however, their compatibility with PDMS coatings for efficient daytime radiative cooling has not been systematically evaluated. More importantly, highly transparent substrates that allow sunlight to pass through, rather than reject it, present opportunities for hybrid solar utilization, where radiative cooling can be combined with downstream use of transmitted sunlight, such as photovoltaic electricity generation [19], solar-thermal collection, daylighting [14], or photosynthesis [14,20]. However, their impact on the overall cooling performance of PDMS-based transparent PDRC systems has not been clearly quantified.

In this study, we conduct a comprehensive evaluation of flat PDMS films as simple PDRC materials on two types of different substrates. PDMS layers with thicknesses of 1.7 μm, 8.3 μm, 58 μm, 121 μm, 317 μm, and 1042 μm were coated onto highly-transparent polished, fused silica wafers, relevant for hybrid solar utilization and PDRC. PDMS layers with thicknesses of 1.8 μm, 8.4 μm, 60 μm, 116 μm, 550 μm, 1002 μm were coated on the highly-reflective commercial sunlight reflectors, relevant for solely cooling applications. We further examine the effect of different mixing ratios of PDMS base to curing agent on optical properties. Measured transmittance, reflectance, and emissivity spectra are used to calculate the cooling power of each configuration. The study provides a systematic dataset and physical insight for the design and optimization of PDMS based PDRC materials.

2. Methodology

We investigated two types of PDMS based PDRC materials, as illustrated in Fig. 1. In both configurations, the upper layer consists of a flat PDMS film, while the underlying substrate is either a highly-transparent silica wafer (Fig. 1a) or a highly-reflective commercial sunlight reflectors (Fig. 1b). Both sample types aim at exhibiting strong thermal emission in the 8–13 μm atmospheric window, which is essential for passive radiative cooling. The transparent configuration (Fig. 1a) allows the incident sunlight to pass through the PDMS layer and the silica substrate. This enables additional functionalities such as daylighting or integration with photovoltaic or hybrid solar systems, where transmitted solar radiation can be utilized downstream. In contrast, the reflective configuration (Fig. 1b) uses a sunlight reflector that reflects nearly all incident sunlight. This design is intended solely for PDRC, as the sunlight reflector prevents solar transmission and promotes a high solar reflectance, which helps reduce solar heating [21]. These two configurations allow us to systematically compare how the substrate, together with PDMS thickness, affects the optical response and cooling performance of simple PDMS based radiative cooling materials.

2.1. Experimental method

Fig. 2 illustrates the fabrication procedure for the PDMS based PDRC samples. First, the PDMS base and curing agent (Sylgard 184, Sigma Aldrich) [22,23] were mixed at a weight ratio of 10:1 in a clean beaker and stirred for 1 min. In the second step, the mixture was degassed in a vacuum oven at room temperature (Thermo Scientific VT 6060 M). The oven was initially operated in vacuum mode, during which air bubbles formed and rose through the liquid. After the bubbles reached the surface, the vacuum pump was switched off while maintaining the vacuum environment until all trapped bubbles were removed. This degassing step typically required 12–15 min (depending on the amount of PDMS) and was necessary to prevent optical scattering or defects in the cured PDMS film. Degassing removes trapped air bubbles from the PDMS base/curing-agent mixture before coating and curing. Since this study focuses on the PDRC performance of pure PDMS coatings without micro-pores on different substrates, removing air bubbles is necessary to avoid

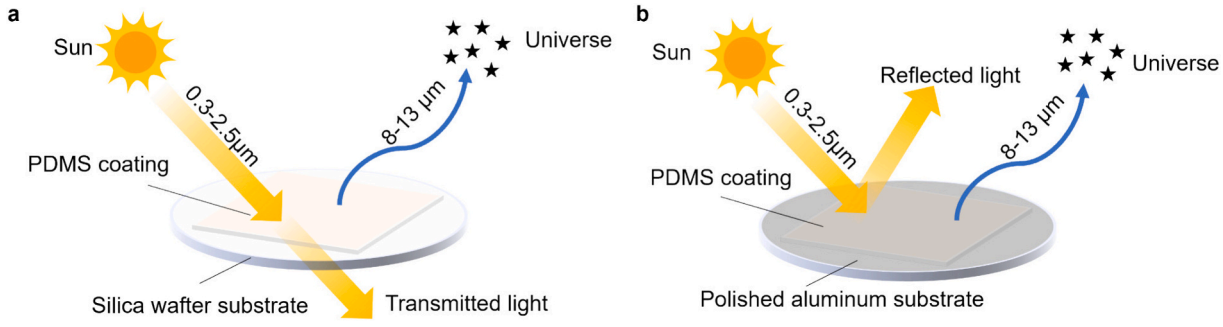

Fig. 1. Diagram of PDMS-based PDRC materials. (a) High-transparent PDRC materials by coating PDMS on a silica substrate, and (b) High-reflective PDRC materials by coating PDMS on a commercial sunlight reflector.

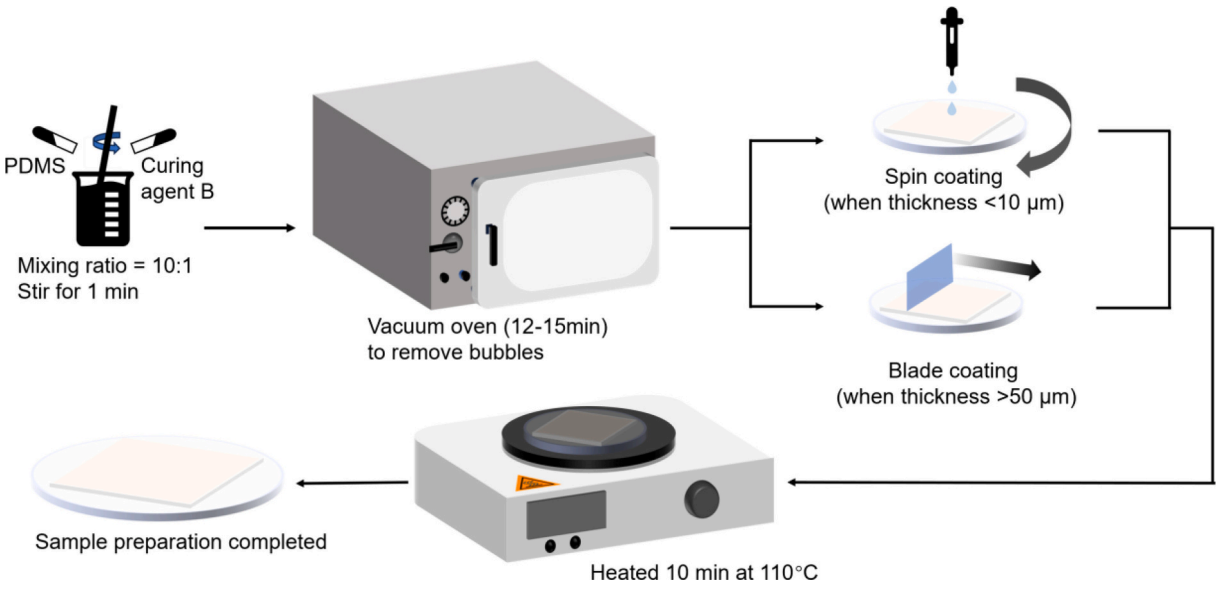

Fig. 2. Schematic illustration of fabrication process of PDMS-based PDRC materials. The PDMS is coated on a substrate *via* spin coating, blade coating, depending on the thickness.

unintended voids and optical scattering in the cured PDMS layer. In the third step, the degassed PDMS solution was coated onto the two types of substrates: highly-transparent 500 μm-thick fused silica wafers (Wafer Universe) and highly-reflective commercial sunlight reflectors (MIRO-High-Reflective-95, Alanod GmbH, Germany). The commercial sunlight reflector consists of a 300 μm-thick aluminium substrate that provides mechanical support, a 56 μm-thick silver layer serving as the primary reflective component, and an approximately 700 nm-thick TiO_2 coating on the surface to protect the underlying silver layer [24]. The PDMS coating area for all samples in this study was 2 cm × 2 cm. Different coating techniques were used depending on the target film thickness. Spin coating was used to prepare thin and uniform films (<10 μm), blade coating was used for intermediate thicknesses (>50 μm), and mould casting was used for thick PDMS layers (>500 μm). These fabrication methods influence the final film thickness and uniformity, which in turn affect the optical path length, solar absorption, mid-infrared emissivity, and radiative cooling performance of the PDMS-based PDRC materials. Therefore, spin coating was applied to produce thin films of 1.7 μm and 8.3 μm. Blade coating was used for intermediate thicknesses of around 60 μm and around 120 μm. For the thickest samples (around 1000 μm), the PDMS mixture was deposited in a mould with the corresponding thickness and then use the blade to smoothen the surface. After coating, all samples were thermally cured at 110 °C for 10 min to complete crosslinking.

The optical properties were measured across the solar and mid infrared ranges. Reflection and transmission spectra from 300 to 2500 nm were obtained using a ultraviolet-visible-near infrared (UV–Vis-NIR) spectrophotometer (Agilent Cary 7000) equipped with an integrating sphere that collects both specular and diffuse components. The mid-infrared emissivity was measured using a Fourier transform infrared spectrometer (Bruker Vertex 70) coupled with an A562 integrating sphere coated with gold to provide a highly reflective surface in the infrared region.

2.2. Numerical method

In this study, we use the same numerical model as Raman et al. [11,25,26] to evaluate the radiative cooling performance of the PDMS based materials. The net cooling power of a PDRC surface is determined by the balance among several radiative and non-radiative heat exchange processes. The material emits thermal radiation (P_{rad}), while it also absorbs part of the incoming radiation from the sun (P_{sun}) and from the atmosphere (P_{atm}). In addition, the non-radiative heat transfer from the surrounding air (P_{con}) must also be considered, as it accounts for both conductive and convective heat exchange with the ambient environment. Therefore, the overall net cooling power (P_{cool}) can be expressed as the difference between the emitted flux and the absorbed fluxes [11]:

$$P_{cool} = P_{rad} - P_{sun} - P_{atm} - P_{con} \tag{1}$$

If the angular distribution of emission is considered, P_{rad} is calculated as[27]:

$$P_{rad} = \int_0^{2\pi} \int_0^{\frac{\pi}{2}} \int_{\lambda_a=0.3\ \mu m}^{\lambda_b=20\ \mu m} I_{bb}(\lambda, T_{rc}) \varepsilon_{rc}(\lambda, \theta) \cos\theta \sin\theta \, d\phi \, d\lambda \, d\theta \tag{2}$$

In most spectral and directional analyses, azimuthal dependence is assumed to be uniform. This allows the azimuthal integral to be simplified to a factor of 2π, giving [11]:

$$P_{rad} = \int_0^{\frac{\pi}{2}} \int_{\lambda_a=0.3\ \mu m}^{\lambda_b=20\ \mu m} I_{bb}(\lambda, T_{rc}) \varepsilon_{rc}(\lambda, \theta) \cos\theta \sin\theta d\lambda \, d\theta \bullet 2\pi \tag{3}$$

Here, θ is the polar angle, $\varepsilon_{rc}(\lambda,\theta)$ is the spectral emissivity of the PDRC material, and $I_{bb}(\lambda,T_{rc})$ is the blackbody spectral radiance at temperature T_{rc}. The function I_{bb} is defined by Planck's law [11]:

$$I_{bb}(\lambda, T_{rc}) = \frac{2hc^2}{\lambda^5} \frac{1}{\exp\left(\frac{hc}{\lambda k_B T_{rc}}\right) - 1} \tag{4}$$

where h is Planck's constant, c is the speed of light, and k_B is the Boltzmann constant.

The absorbed solar radiation P_{sun} is calculated over the wavelength range of 0.3–2.5 μm, corresponding to the air mass 1.5 global (AM1.5G) solar spectrum. $I_s(\lambda)$ is the solar irradiance, and $\varepsilon_{rc}(\lambda,\theta_{sun})$ is the spectral absorptance of the material at the solar incidence angle. In this work, normal incidence is assumed ($\theta_s = 0$) [11]:

$$P_{sun} = \int_{0.3\ \mu m}^{2.5\ \mu m} I_s(\lambda) \varepsilon_{rc}(\lambda, \theta_{sun}) d\lambda \tag{5}$$

The atmospheric thermal radiation absorbed by the surface, P_{atm}, is given by[27]:

$$P_{atm} = \int_0^{\frac{\pi}{2}} \int_{\lambda_a}^{\lambda_b} I_{bb}(\lambda, T_a)\varepsilon_{rc}(\lambda,\theta)\varepsilon_{atm}(\lambda,\theta)\cos\theta\sin\theta d\lambda\, d\theta \bullet 2\pi \quad (6)$$

where T_a is the ambient temperature. The atmospheric emissivity $\varepsilon_{atm}(\lambda,\theta)$ is calculated from the atmospheric transmittance $\tau_{atm}(\lambda)$ as[27]:

$$\varepsilon_{atm}(\lambda,\theta) = 1 - \tau_{atm}(\lambda)^{1/\cos\theta} \quad (7)$$

The transmittance spectrum $\tau_{atm}(\lambda)$ used in this study is based on the US Standard Atmosphere model. Non-radiative heat transfer between the ambient air and the PDRC surface consists of convection and conduction, represented by P_{con}. It is expressed as[27]:

$$P_{con} = h_c(T_a - T_{rc}) \quad (8)$$

where h_c is the convective heat transfer coefficient and we use 5 W/m^2/K in this study. It should be noted that the present numerical model does not involve fluid flow. Instead, it is based on an energy balance for radiative cooling, which accounts for thermal radiation emitted by the PDRC surface, absorbed solar radiation, absorbed atmospheric radiation, and non-radiative heat exchange with the ambient environment. Therefore, fluid-flow governing equations, such as vector-form momentum equations, are not applicable to this study.

3. Results and discussion

3.1. Optical properties of base materials of silica, sunlight reflector and PDMS

To evaluate the optical and radiative behaviour of the double-layer PDRC materials shown in Fig. 1, the optical properties of the base materials, namely silica wafter, sunlight reflector, and PDMS, were first characterized. In addition, the intrinsic optical properties of PDMS were examined by measuring a freestanding 60-μm-thick PDMS film without any substrate. This baseline characterization is essential for understanding the individual optical contributions of each layer and for interpreting the performance of the combined PDMS based PDRC structures.

The silica wafer exhibits a high and spectrally uniform transmittance across the solar spectrum from 0.3 to 2.5 μm, as shown in Fig. 3(a), indicating minimal solar absorption loss. In the mid-infrared region, particularly within the 8 to 13 μm atmospheric transparency window, the silica wafer shows a valley in absorption. This characteristic implies that, while silica is advantageous for solar transmission, additional effort is needed to improve the absorption in the mid-infrared region for PDRC.

The commercial sunlight reflector demonstrates a high reflectance throughout the solar spectrum, as shown in Fig. 3(b), which is beneficial for suppressing solar heating in reflective PDRC configurations. The sunlight reflector absorbs a part of the UV spectrum (<400 nm). In the mid-infrared range, the sunlight reflector maintains very low emissivity, or equivalently very high reflectance, consistent with the expected optical behaviour of metallic reflectors. As a result, the sunlight reflector itself contributes negligibly to thermal radiation and primarily serves as an optical backing layer that reflects incident radiation back into the overlying PDMS layer, thereby modifying the effective optical path length and emission characteristics of the coating.

Fig. 3(c) presents the measured spectral properties of a 60-μm-thick freestanding PDMS film. PDMS shows high transmittance across the solar spectrum, confirming its suitability for minimizing solar absorption. In contrast, pronounced absorption bands are observed in the mid-infrared region, particularly within and beyond the 8 to 13 μm atmospheric window. These absorption features originate from vibrational modes of the Si–O–Si backbone and the Si–CH_3 groups (more details will be provided in the next section), and they directly correspond to strong thermal emission according to Kirchhoff's law. This combination of low solar absorption and high mid-infrared emissivity highlights PDMS as an intrinsically suitable material for passive daytime radiative cooling applications.

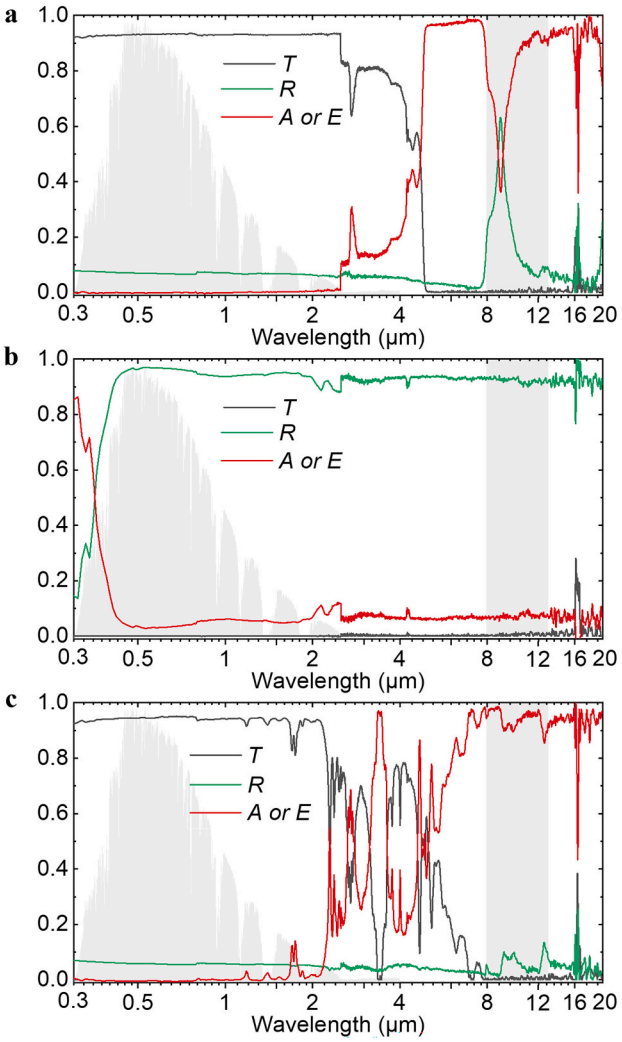

Fig. 3. Transmittance (T), reflectance (R) and absorption (A or E) of different base materials. (a) 0.5-mm-thick silica wafer, (b) commercial sunlight reflector, (c) 60-μm-thick PDMS film.

3.2. High-transparent PDMS-based PDRC materials

3.2.1. Optical properties of a highly-transparent sample with 58-μm-thickness PDMS coating

We first analyze the optical properties of the high transparent PDMS based PDRC sample with a 58 μm-thick PDMS coating, as shown in Fig. 4 (a). As expected, the sample appears visibly transparent. Fig. 4(b) presents the measured transmittance (*T*), reflectance (*R*), and absorption (*A* or *E*) spectra of the sample over the wavelength range of 0.3–16 μm. The region from 0.3 to 2.5 μm corresponds to the solar spectrum, while the range from 8 to 13 μm represents the atmospheric transparency window relevant to radiative cooling. The sample exhibits a high transmittance of 92.8% and a low absorption of 1.1% in the solar spectrum, which helps minimize solar heating. In the mid infrared range, the sample shows a strong emissivity of 94.4% within the 8–13 μm atmospheric window, which is essential for achieving effective PDRC while allowing sunlight to pass through for potential downstream solar utilization.

This combination of high solar transmittance, low solar absorption, and high mid-infrared emissivity is particularly important for transparent PDRC applications. The high solar transmittance allows most incident sunlight to pass through the PDMS/silica sample, while the low

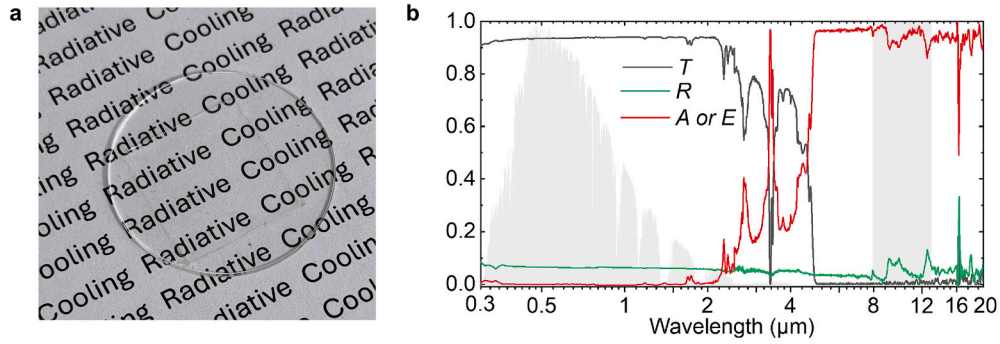

Fig. 4. An image and optical properties of high-transparent PDMS-based PDRC samples. (a) Optical image of a 58 μm-thick PDMS film coated on a high-transparency silica wafer. (b) Optical properties of a 58 μm-thick PDMS film sample, including transmittance, reflectance and absorption spectra.

solar absorption minimizes solar heating of the cooling surface. Meanwhile, the strong emissivity in the 8–13 μm atmospheric window enables efficient thermal radiation to outer space. Together, these optical properties allow the transparent PDMS-based PDRC sample to achieve effective radiative cooling while simultaneously transmitting sunlight for potential downstream solar energy utilization, such as such as photovoltaic or photosynthesis [19,20].

As shown in Fig. 4(b), several distinct absorption peaks appear across the infrared spectrum. To understand the origin of these peaks, it is necessary to consider the molecular structure of PDMS. PDMS has the repeating chemical structure $[-Si(CH_3)_2 - O-]_n$, which contains Si–O–Si backbone bonds, Si–CH_3 groups that include C—H bonds, and CH_3 (methyl) side groups [27,28]. These functional groups generate multiple characteristic vibrational modes, each associated with specific infrared absorption wavelengths. Table 1 summarizes the main absorption features observed in the PDMS sample, including their wavelengths, vibration types, underlying mechanisms, and molecular origins [29–33].

3.2.2. Impact of PDMS layer thickness on optical properties of high-transparent PDMS-based PDRC materials

To investigate the impact of PDMS layer thickness on the optical properties of the highly- transparent PDMS-based PDRC materials, six samples with thicknesses of 1.7 μm, 8.3 μm, 58 μm, 121 μm, 317 μm, and 1042 μm were fabricated. Their measured optical spectra are shown in Fig. 5(a)–(f). The corresponding average transmittance and absorptance in the solar spectrum (0.3–2.5 μm), as well as the average emissivity in the 8–13 μm range, are summarized in Fig. 5. Weak interference oscillations can be observed in some spectra, such as in Fig. 5a for the 1.7 μm-thick PDMS layer. These oscillations originate from thin-film interference within the PDMS layer. Since the experimentally measured spectra were directly used in the cooling-power calculation, the influence of these interference features is already included in the spectral integration."

Table 1
Summary of spectral absorption peaks in the PDMS, including wavelength, absorption type, vibrational mode/mechanism, and origin.

Wavelength (μm)	Absorption type	Vibration mode/Mechanism
0.25–0.4	Electronic transition	$\pi \rightarrow \pi^*$, $n \rightarrow \pi^*$ electronic transitions in Si—O and C—H bonds
1.7	1st overtone	C–H stretching overtone ($v = 0 \rightarrow 2$), mainly from CH_3 groups
2.3	Combination	Combination band: C—H stretching + CH_3 bending (Si–CH_3 deformation)
2.7	Fundamental	O–H stretching from adsorbed H_2O or Si–OH groups
3.4	Fundamental	C–H stretching (symmetric/asymmetric) in Si–CH_3
4.58	Fundamental	Si–C skeletal stretching with CH_3 deformation coupling
4.9	Fundamental	Coupled Si—C stretching and CH_3 bending in PDMS network
7.5–8.5	Fundamental	CH_3 symmetric bending (in-plane rocking of Si–CH_3)
9.1	Fundamental	Si–O–Si asymmetric stretching in siloxane network
9.8	Fundamental	Si–O–Si symmetric stretching in siloxane network
~12.5	Fundamental	Si–O bending (rocking) and network deformation

In the solar spectrum region (0.3–2.5 μm), all samples exhibit consistently high transmittance, indicating that PDMS remains an excellent solar transparent material even when its thickness varies over three orders of magnitude. The absorption in the UV region (<400 nm) is negligible for all thicknesses from 1.7 μm to 1042 μm, as PDMS has no strong electronic absorption bands in this wavelength range. Several small absorption peaks appear in the near infrared region between 1.1 and 2 μm, and these peaks become more pronounced with increasing PDMS thickness due to the longer optical paths within the material. A high transmittance and low absorptance are desired in this range to minimize solar heating. As summarized in Fig. 6(a), increasing the PDMS thickness from 1.7 μm to 1042 μm decreases the average transmittance from 93.7% to 91.5%, while the average absorption increases from nearly 0% to 2.3%. It is notable that the samples with thicknesses of 1.7 μm, 8.3 μm, and 58 μm exhibit almost identical transmittance and absorptance.

For the absorption (emissivity) in the 8–13 μm atmospheric window, the sample with 1.7 μm PDMS shows a noticeable dip around 8 μm, as seen in Fig. 6(b). This is due to insufficient optical thickness in the mid infrared range, which prevents the intrinsic vibrational absorption modes of PDMS from reaching their full emissive potential. When the PDMS thickness increases to 8.3 μm, the emissivity improves significantly, and as the thickness increases further to 58 μm and above, the emissivity spectra become almost identical. As summarized in Fig. 6(b), the average emissivity increases from 89.8% at 1.7 μm to 94.2% at 1042 μm, with saturation occurring at 58 μm and beyond. A high emissivity in the 8–13 μm range is essential for maximizing radiative cooling power, and these results confirm that a PDMS thickness of at least 58 μm is required for the emissivity to reach its full potential. Measurement uncertainty of the spectrophotometer and FTIR was evaluated by performing ten repeated measurements. The standard deviation of the transmittance and emissivity measurements were estimated to be ±0.4% and ± 0.1% (absolute value), respectively.

3.3. High-reflective PDMS-based PDRC materials

To investigate the impact of PDMS layer thickness on the optical properties of the high reflective PDMS based PDRC materials, six samples with PDMS thicknesses of 1.8 μm, 8.4 μm, 60 μm, 116 μm, 550 μm, and 1002 μm were fabricated. Their optical spectra are shown in Figs. 7 (a)–(f), and the corresponding average transmittance, absorptance in the

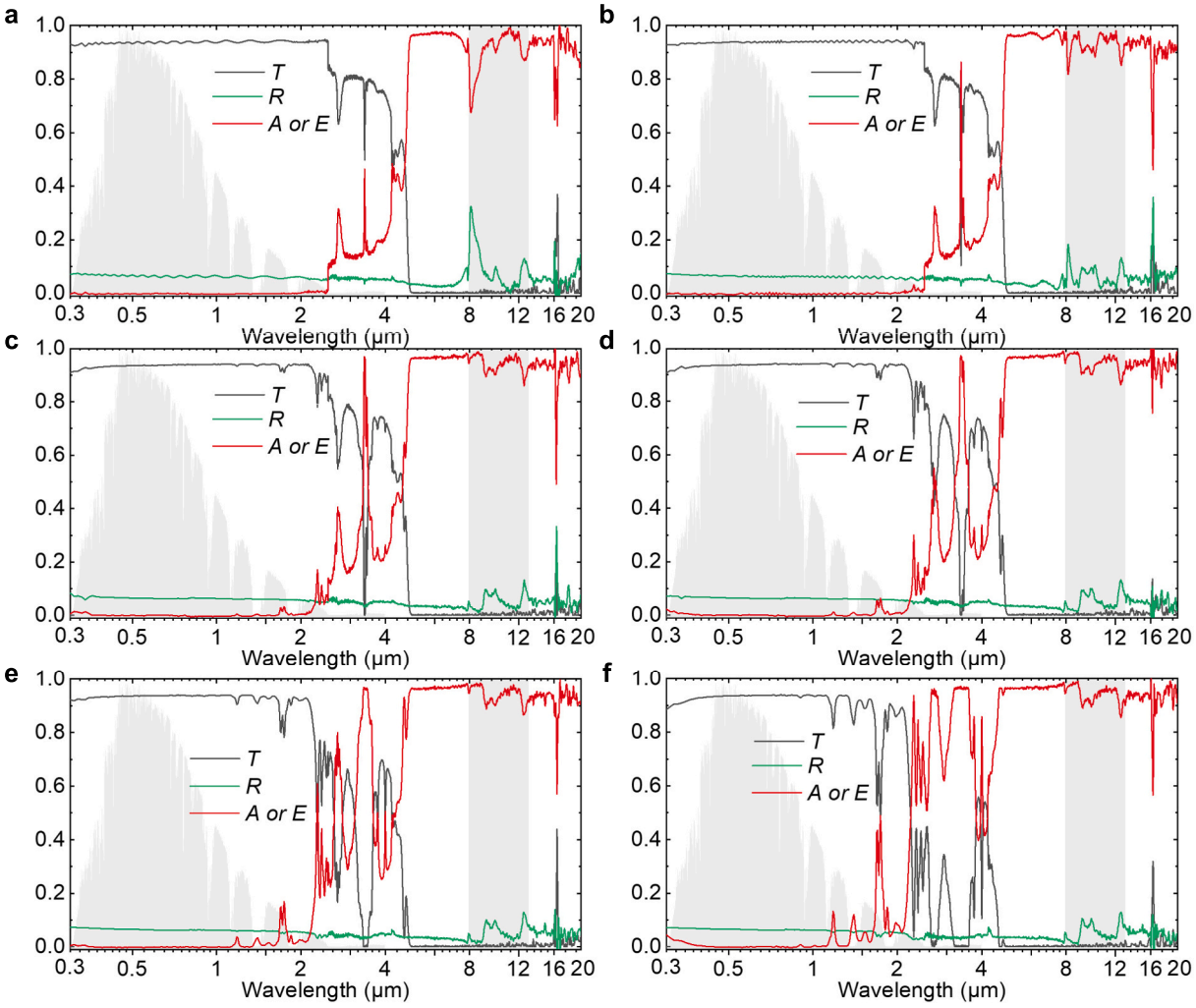

Fig. 5. Transmittance (T), reflectance (R) and absorption (A or E) spectra of PDMS films with different thicknesses coated on a silica substrate. Optical spectra with different PDMS thicknesses of (a) 1.7 μm, (b) 8.3 μm, (c) 58 μm, (d) 121 μm, (e) 317 μm, and (f) 1042 μm.

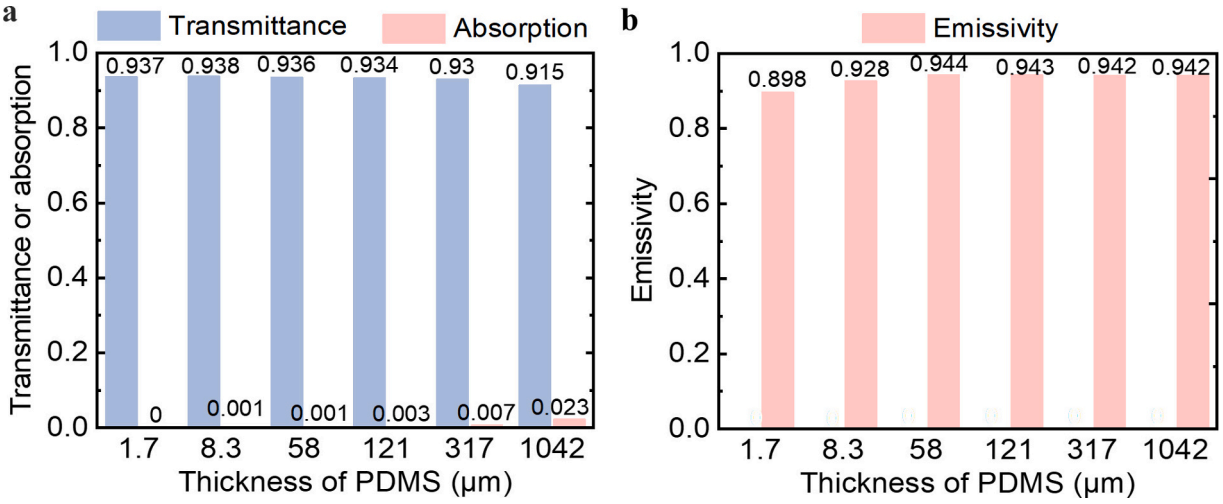

Fig. 6. Spectral-weighted average transmittance, absorptance and emissivity of PDMS films with different thicknesses coated on a silica substrate. (a) Average transmittance and absorptance of PDMS films with various thicknesses in the wavelength range of 0.3–2.5 μm. (b) Average emissivity of PDMS films with different thicknesses in the wavelength range of 8–13 μm.

solar spectrum (0.3–2.5 μm), and average emissivity in the 8–13 μm range are summarized in Fig. 8.

In the solar spectrum range (0.3–2.5 μm), all samples exhibit high overall reflectance because the sunlight reflector reflects most of the

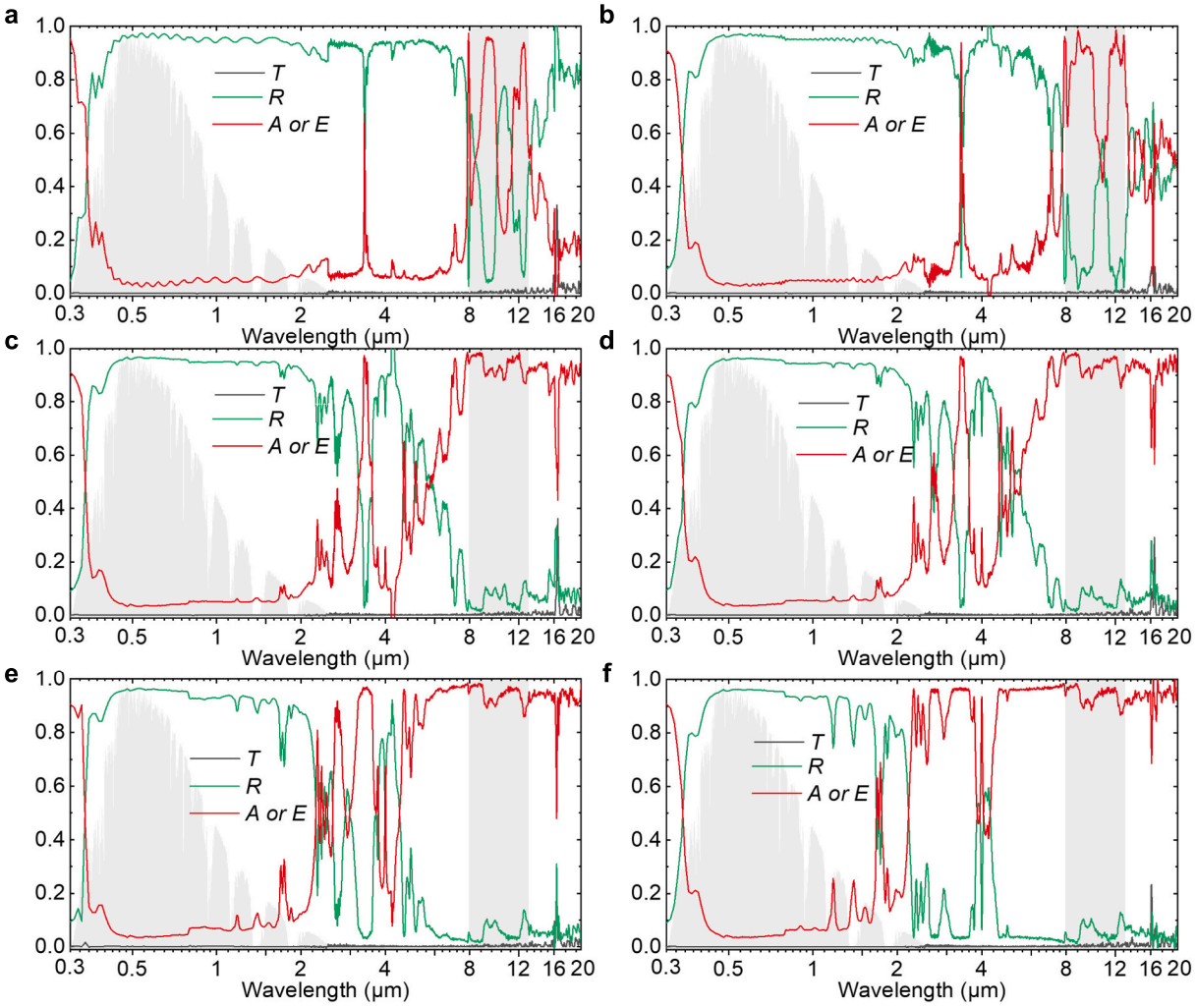

Fig. 7. Transmittance (T), reflectance (R) and absorption (A or E) spectra of PDMS films with different thicknesses coated on a commercial sunlight reflector substrate. Optical spectra with different PDMS thicknesses of (a) 1.8 μm, (b) 8.4 μm, (c) 60 μm, (d) 116 μm, (e) 550 μm, and (f) 1002 μm.

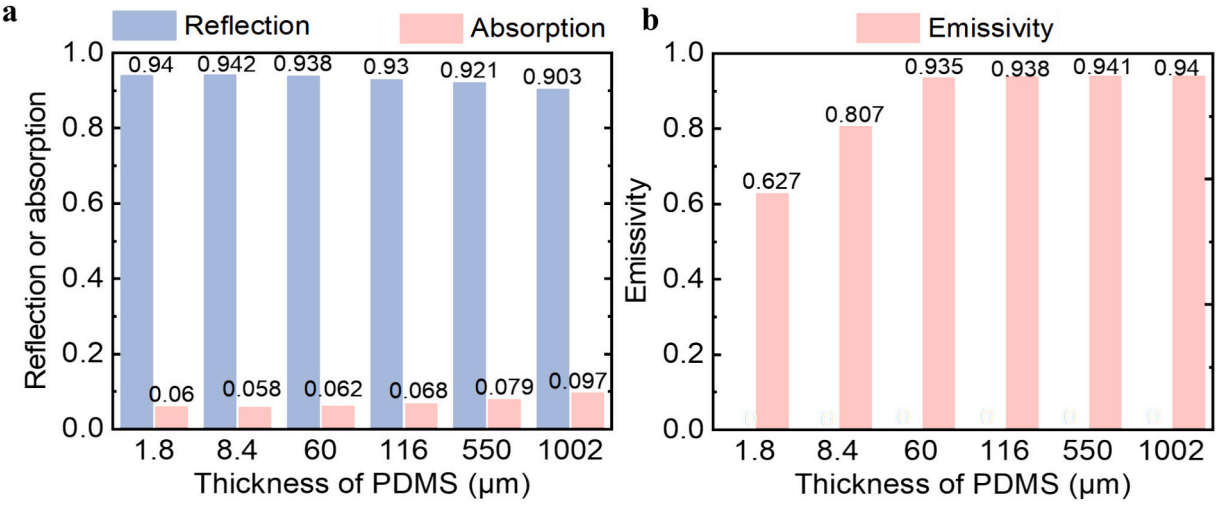

Fig. 8. Spectral-weighted average transmittance, absorptance and emissivity of PDMS films with different thicknesses coated on a commercial sunlight reflector substrate. (a) Average transmittance and absorptance of PDMS films with various thicknesses in the wavelength range of 0.3–2.5 μm. (b) Average emissivity of PDMS films with different thicknesses in the wavelength range of 8–13 μm.

incoming sunlight. All samples have UV absorption in <400 nm range due to the commercial sunlight reflector absorbs a portion of the UV spectrum. Several small absorption peaks appear between 1.1 μm and 2 μm, and these peaks become more pronounced as the PDMS thickness

increases. Compared to the high transparent samples, the high reflective samples display more significant absorption in the solar spectrum. This increase originates from two physical mechanisms: i) silver has a higher intrinsic absorption than silica in the solar spectrum; and ii) sunlight entering the PDMS layer undergoes multiple reflections between the PDMS film and the sunlight reflector substrate, effectively increasing the optical path length inside the PDMS layer. This enhances the probability of absorption, making even moderate PDMS thicknesses behave optically thicker in the near infrared region.

To minimize solar heating, high reflectance and low absorptance are required in this spectral range. As summarized in Fig. 8(a), increasing the PDMS thickness from 1.8 μm to 1002 μm reduces the average reflectance from 94.0% to 90.3% and increases the average absorption from 6.0% to 9.7%. These trends confirm that thicker PDMS layers significantly increase solar absorption on reflective substrates.

For the absorption (emissivity) in the 8–13 μm atmospheric window, the samples with thin PDMS layers (1.8 μm and 8.4 μm) exhibit selective emission, meaning that the emissivity is high within the 8–13 μm window while remaining low in the rest of the mid infrared region, as shown in Figs. 7(a) and (b). This selective emission occurs because the sunlight reflector has very low absorption across the mid infrared range, so the overall emission spectrum is dominated by the PDMS layer alone. In contrast, in the high transparent samples with silica substrates, the silica itself absorbs broadly in the mid infrared, so the selective emission behaviour cannot be observed at similar PDMS thicknesses. When the PDMS thickness increases to 60 μm, the emissivity increases substantially, and for thicknesses above 60 μm, the emissivity spectra become nearly identical. This indicates that beyond an optical thickness of 60 μm, the PDMS layer becomes thick enough that the emitted infrared radiation is determined solely by intrinsic vibrational absorption modes of PDMS, and further thickness no longer enhances emissivity. As summarized in Fig. 8(b), the average emissivity increases from 62.7% at 1.8 μm to 94.0% at 1002 μm, with saturation occurring at 60 μm and above. A high emissivity in the 8–13 μm atmospheric window is critical for achieving strong PDRC performance. For a clear comparison of the two types of samples with different PDMS thicknesses, the spectral-weighted average optical properties are summarized in Fig. 9. Fig. 9 (a) shows the average transmittance, reflectance and absorptance in the solar spectrum range, while Fig. 9(b) shows the average emissivity in the 8–13 μm atmospheric window.

Overall, for the high-reflective PDMS based PDRC samples, increasing the PDMS thickness results in two competing effects: the solar absorption increases significantly, leading to higher solar heating, while the mid infrared emissivity also increases, enhancing radiative cooling. Therefore, an optimal optical thickness must exist to balance these effects. Identifying such a thickness is essential for designing PDMS based PDRC systems on reflective substrates. We also checked the cross-sectional Scanning Electron Microscopy (SEM) image of the PDMS-coated substrate as shown in Fig. 10. The SEM image was taken for the thin 8-μm-thick PDMS coating, because the performance of thin coatings are more sensitive to potential interfacial defects and micro-voids. The image shows that the PDMS coating forms a continuous layer on the substrate, without obvious large voids, cracks, or interfacial defects in the observed region. The absence of visible voids is also consistent with the degassing step used during fabrication, which removes trapped air bubbles before coating and curing. It should be noted that the SEM image only shows a selected region of the sample, because high magnification is required to clearly observe the coating structure. For the rest of the sample area, the same degassed PDMS mixture was used, and no visible bubbles were observed during preparation. The same coating method was also applied across the full sample area, supporting similar coating structures. Moreover, the optical measurements provide an area-averaged characterization of the samples.

3.4. Cooling power analysis of PDMS-based high-transparent and high-reflective PDRC materials

Based on the previous analysis, the thickness of the PDMS layer introduces a clear trade-off between solar absorption and thermal radiation. Therefore, to determine the optimal PDMS thickness for PDRC applications, it is necessary to simulate and calculate the net cooling power for samples with different thicknesses. Figs. 11(a)–(d) presents net cooling power of PDMS films with different thicknesses coated on

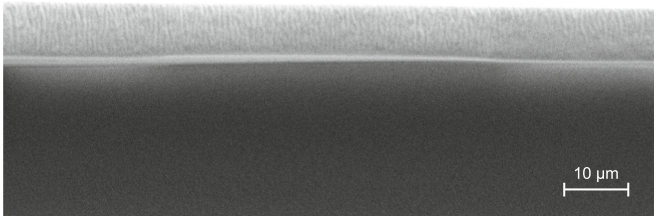

Fig. 10. Cross-sectional Scanning Electron Microscopy (SEM) image of the PDMS-coated substrate. The image shows a continuous PDMS layer on the substrate without obvious micro-voids, cracks, or interfacial defects in the observed region.

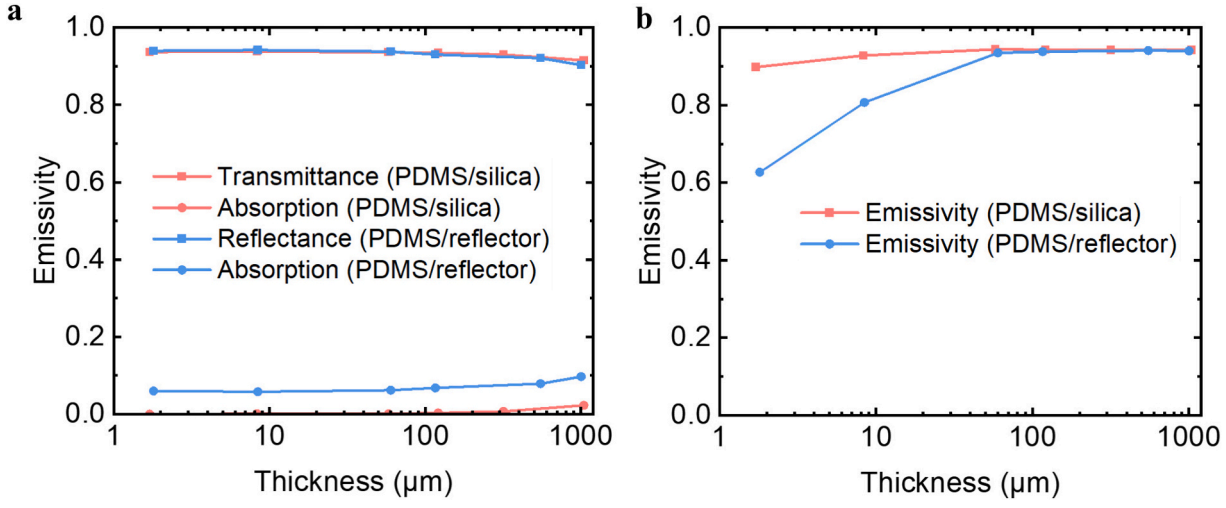

Fig. 9. Comparison of the transparent configuration (PDMS/silica) and the reflective configuration (PDMS/reflector). (a) Average transmittance, reflectance, and absorptance in the solar spectrum range of 0.3–2.5 μm. (b) Average emissivity in the atmospheric transparency window of 8–13 μm.

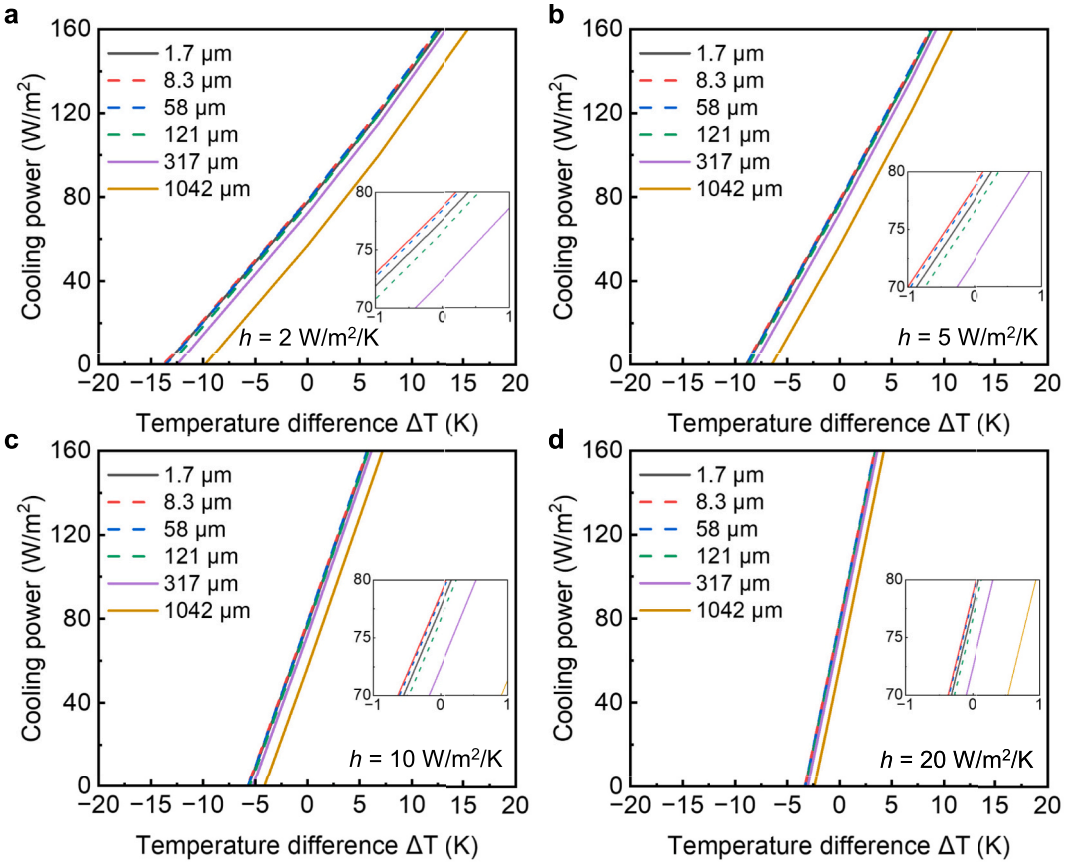

Fig. 11. Net cooling power of PDMS films with different thicknesses coated on silica wafers under different convective heat transfer coefficients: (a) $h = 2$ W/m^2/K, (b) $h = 5$ W/m^2/K, (c) $h = 10$ W/m^2/K and (d) $h = 20$ W/m^2/K.

silica wafers under different convective heat transfer coefficients of $h =$ 2, 5, 10, 20 W/m^2/K. Fig. 11(b) presents the net cooling power of the high transparent PDRC samples as a function of temperature difference (*i.e.*, PDRC sample temperature minus ambient temperature), under a convective heat transfer coefficient of $h = 5$ W/m^2/K. All samples with different PDMS thicknesses can achieve sub ambient cooling, indicating that the silica substrate combined with PDMS provides a favourable optical platform for daytime radiative cooling.

The cooling power curves for PDMS thicknesses between 1.7 μm and 121 μm are nearly identical, with only minor differences. This is because PDMS in this thickness range maintains high solar transmittance (low solar absorption) and sufficiently high mid infrared emissivity, leading to similar radiative performance. In contrast, the 1042 μm PDMS sample exhibits significantly reduced cooling power. This reduction is attributed to the much higher solar absorption of the thick PDMS layer, which overwhelms the benefit of increased mid infrared emissivity. The minimum achievable temperature for the high transparent samples is around 8–9 °C below the ambient temperature, suggesting strong cooling potential when a transparent substrate is used. When the convective heat transfer coefficient increases, as shown in Fig. 11, the sub-ambient cooling performance decreases due to the stronger heat gain from the ambient environment. Therefore, wind shielding and thermal insulation are important for maintaining high cooling performance. However, the convective heat transfer coefficient does not change the optimal PDMS coating thickness, as it affects the overall heat exchange with the ambient environment rather than the optical trade-off between solar absorption and mid-infrared emission.

Figs. 12(a)–(d) presents net cooling power of PDMS films with different thicknesses coated on sunlight reflectors under different convective heat transfer coefficients of $h = 2$, 5, 10, 20 W/m^2/K. In contrast to the high transparent samples, the high reflective samples experience difficulty achieving effective sub ambient cooling. This is mainly due to the substantially higher solar absorption arising from the sunlight reflector and the enhanced internal reflection within the PDMS layer. Especially for very thin PDMS (1.8 μm) or very thick PDMS (1002 μm), the cooling performance becomes extremely poor. Although commercial sunlight reflectors are cost-effective and widely available, their relatively high solar absorption makes it challenging to achieve efficient daytime radiative cooling without additional design considerations. When the convective heat transfer coefficient changes from 2 to 20 W/m^2/K, as shown in Fig. 12, the reflective PDRC samples still cannot provide effective sub-ambient cooling because of the aforementioned solar heating issue.

The detailed values of thermal emission from the PDRC sample (P_{rad}), thermal absorption from the atmosphere (P_{atm}), solar absorption (P_{sun}), and net cooling power (P_{cool}) at zero temperature difference (PDRC sample temperature is the same as the ambient temperature) are summarized in Table 2. When the system operates at zero temperature difference, the conductive and convective heat exchange with the ambient air (P_{con}) is zero by definition, and therefore it is not listed in the table. The data clearly show that the high transparent samples maintain low solar absorption across a broad thickness range, whereas the high reflective samples exhibit much higher solar absorption and consequently lower P_{cool}.

For the high transparent PDRC samples, the cooling power curves for PDMS thicknesses from 1.7 μm to 121 μm differ by less than 3%. This indicates that, from a cooling power perspective, any PDMS thickness below 121 μm is suitable. For practical fabrication, using thinner coatings reduces material consumption and curing time, while still ensuring high cooling performance. Thicknesses greater than approximately 1.7 μm are generally sufficient to achieve saturated mid infrared emissivity while maintaining excellent solar transparency. Overall, the high

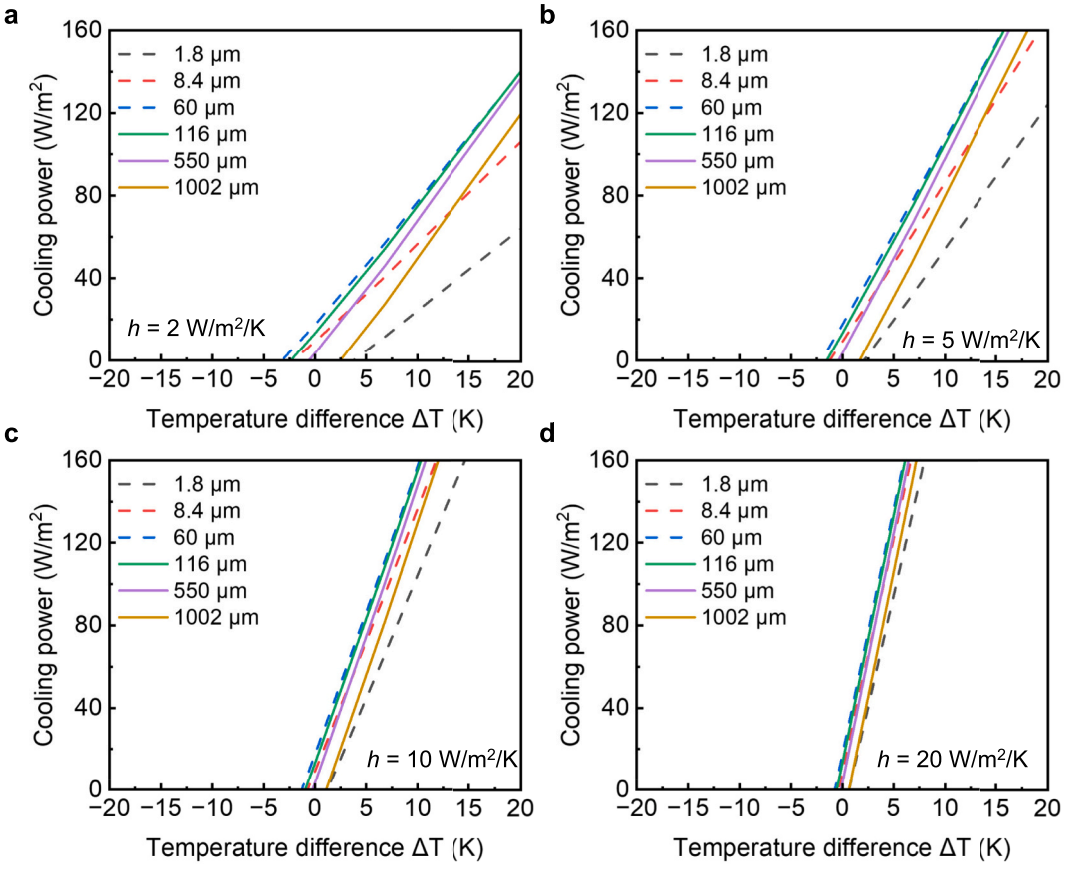

Fig. 12. Net cooling power of PDMS films with different thicknesses coated on sunlight reflectors under different convective heat transfer coefficients: (a) $h = 2$ W/m^2/K, (b) $h = 5$ W/m^2/K, (c) $h = 10$ W/m^2/K and (d) $h = 20$ W/m^2/K.

Table 2
Calculated values of P_{rad}, P_{atm}, P_{sun} and P_{cool} for PDMS films on silica wafers and sunlight reflector substrates of different thicknesses at $\Delta T = 0$.

PDMS thickness (μm)	Highly-transparent samples (PDMS on silica)				PDMS thickness (μm)	Highly-reflective samples (PDMS on sunlight reflector)			
	Psun (W/m^2)	Prad (W/m^2)	Patm (W/m^2)	Pcool (W/m^2)		Psun (W/m^2)	Prad (W/m^2)	Patm (W/m^2)	Pcool (W/m^2)
1.7	0.28	248.2	170.3	77.5	1.8	59.3	106.9	61.4	−13.9
8.3	0.59	250.0	170.7	78.7	8.4	56.7	164.0	97.9	9.2
58	2.04	254.3	173.9	78.4	60	61.1	236.0	157.3	17.5
121	3.67	254.7	174.4	76.5	116	67.7	244.3	163.3	13.2
317	8.19	253.6	173.1	72.3	550	76.6	252.6	172.4	3.6
1042	23.32	254.3	174.0	57.0	1002	95.6	255.0	174.8	−15.4

transparent PDMS based PDRC samples demonstrate strong potential for hybrid solar utilization where both cooling and solar transmission are desired.

For the high reflective PDRC samples, the optimal PDMS thickness is approximately 60 μm, which represents a balance between the competing effects of solar absorption and mid infrared thermal emission. However, even at this thickness, the overall radiative cooling performance remains inferior to that of the high transparent samples due to the intrinsic solar absorptance of the sunlight reflector substrate. Although the commercial sunlight reflector exhibits high reflectance over most of the solar spectrum, it still shows noticeable absorption in the UV region. This behaviour is not caused by the PDMS coating or curing process, since the absorption is already observed for the bare reflector. UV absorption has also been reported for laboratory-fabricated silver-reflector-based radiative cooling samples [18]. In the present commercial reflector, the surface TiO2 protective layer is responsible for this additional UV absorption, which is undesired for PDRC. This intrinsic absorption of the reflector contributes to the relatively high calculated solar absorption of the reflective PDMS-based PDRC samples.

The key difference is that the transparent PDMS/silica configuration maintains very low solar absorption while achieving high mid-infrared emissivity, leading to much higher net cooling power. In contrast, the reflective PDMS/sunlight-reflector configuration shows higher solar absorption due to the reflector substrate and multiple internal reflections within the PDMS layer, which limits its daytime cooling performance even when the emissivity is high. PDMS thickness affects the balance between emissivity and solar absorption. Increasing PDMS thickness enhances mid-infrared emissivity because of stronger vibrational absorption in the 8–13 μm atmospheric window. However, it also increases solar absorption because of the longer optical path length.

The cooling-power calculation in this study assumes normal solar incidence. In actual all-day operation, the solar incident angle changes with time, which can increase the equivalent optical path length in the PDMS layer and may slightly change the solar absorption, especially for

reflective configurations with multiple internal reflections. However, this effect is expected to be limited for the present samples. As shown in Figs. 6 and 8, increasing the PDMS thickness from around 60 μm to around 120 μm, corresponding approximately to a doubled optical path length, increases the solar absorption by only about 0.2% for the transparent configuration and about 0.6% for the reflective configuration. In addition, when the solar elevation angle is low, the incident solar irradiance is also significantly reduced. Therefore, normal solar incidence was used as a reasonable approximation in the present cooling-power calculation.

Overall, PDMS thickness strongly affects the balance between mid-infrared emissivity and solar absorption. Increasing the PDMS thickness enhances absorption/emission in the 8–13 μm atmospheric window due to the intrinsic vibrational modes of PDMS. However, it also increases solar absorption because of the longer optical path length, which can reduce the net cooling power. This trade-off is relatively weak for transparent silica substrates, where solar absorption remains low over a broad thickness range, but becomes more significant for reflective substrates because multiple internal reflections further increase absorption within the PDMS layer.

To improve the cooling power while still using low-cost commercial sunlight reflectors, additional strategies are required. For example, solar shading has been reported as an effective strategy to suppress direct solar heating [15], thereby allowing the device to better utilize its high mid-infrared emissivity. We therefore conducted an additional calculation of the cooling performance when direct solar irradiance is blocked by a sun shield, as shown in Fig. 13. Fig. 13(a) shows the net cooling power of the transparent configuration with solar shading, while Fig. 13 (b) shows the corresponding result for the reflective configuration. Compared with the unshaded case, the influence of PDMS thickness becomes less pronounced under solar shading because the solar absorption term is largely removed from the energy balance. Under this condition, the reflective configuration can also achieve a simulated temperature reduction of approximately 8–9 °C below the ambient temperature, indicating that solar shielding can partially mitigate the limitation caused by solar absorption when direct solar irradiance is blocked in the commercial reflector.

We then conducted outdoor experiments to evaluate the cooling performance of the transparent and reflective configurations under real environmental conditions. Samples with an area of 10 cm × 10 cm were fabricated and placed inside a thermally insulated chamber, as shown in Fig. 14(a). To reduce non-radiative heat exchange with the ambient environment, the chamber was externally covered with 2-cm-thick thermal insulation foam. A low-density polyethylene (LDPE) film was used as the top infrared-transparent wind shield, allowing thermal radiation from the samples to be emitted toward the sky while suppressing convective heat transfer. A 1-mm-thick clear silica plate was placed at the bottom of the chamber to support the samples. The inner side walls of the chamber were covered with solar reflectors to minimize parasitic solar heating from the chamber walls. In addition, an A4-size sunlight reflector was placed vertically as a sun shield to block direct solar irradiance from reaching the samples, while still allowing the samples to radiatively exchange heat with the cold sky.

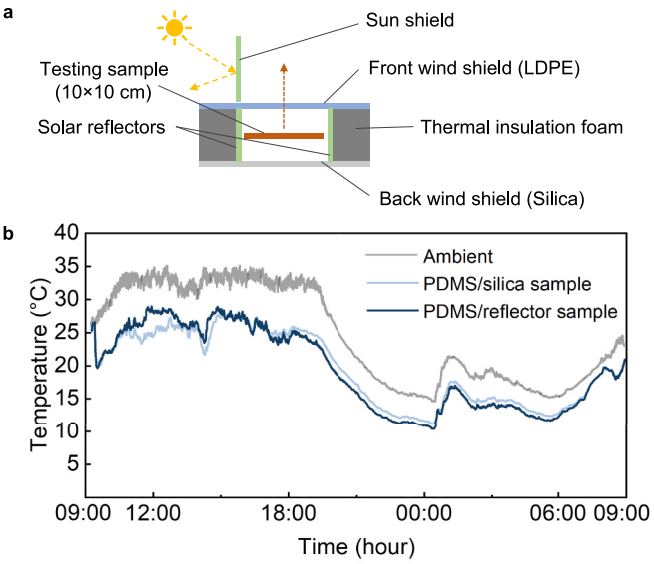

Fig. 14. Outdoor cooling performance of the transparent and reflective PDMS-based PDRC configurations under solar shielding. (a) Schematic illustration of the outdoor testing setup, including a thermally insulated chamber, LDPE infrared-transparent wind shield, solar-reflective inner walls, silica support plate, and sunlight reflector used as a sun shield to block direct solar irradiance. (b) Measured ambient temperature and sample temperatures of the transparent PDMS/silica configuration and reflective PDMS/reflector configuration during a 24-h outdoor test.

Fig. 14(b) shows the measured ambient temperature and the temperatures of the transparent PDMS/silica sample and reflective PDMS/reflector sample during a 24-h outdoor test. Both samples show sub-ambient cooling during daytime and nighttime, confirming that the PDMS-based configurations can provide radiative cooling under real outdoor conditions. During daytime, especially in the afternoon when the relative humidity is lower and the atmospheric transparency window is more effective, both configurations show clear cooling below the ambient temperature. From 12:00 to 18:00 daytime, the transparent PDMS/silica sample and reflective PDMS/reflector sample show average

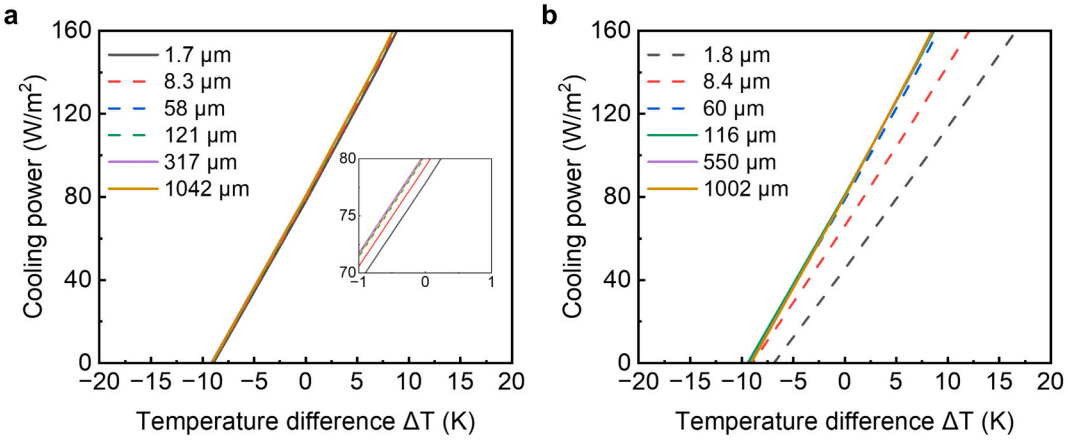

Fig. 13. Net cooling power of the transparent and reflective configurations under solar shielding: (a) transparent configuration with PDMS films coated on silica substrates and (b) reflective configuration with PDMS films coated on sunlight reflectors. The convective heat transfer coefficient is h = 5 W/m^2/K.

temperature reductions of approximately 7.0 °C and 6.4 °C below ambient, respectively. During nighttime, from 21:00 to 05:00, the average temperature reductions below ambient are approximately 3.6 °C and 4.5 °C, respectively. The smaller nighttime cooling temperature is mainly attributed to the higher nighttime humidity, which increases atmospheric infrared emission and weakens radiative heat loss through the atmospheric transparency window.

These outdoor results experimentally confirm the radiative cooling capability of both PDMS-based configurations. The reflective configuration can also achieve sub-ambient cooling when direct solar heating is suppressed by solar shielding, consistent with the numerical analysis. The comparable cooling trends of the transparent and reflective samples indicate that the high mid-infrared emissivity of the PDMS layer plays a dominant role once solar absorption is minimized.

It should be noted that the effectiveness of solar shielding depends on geographic location, solar position, and shielding geometry. In Karlsruhe, the maximum solar elevation angle in summer is around 65°, so a properly positioned vertical sun shield can still block direct solar irradiance around midday, which is consistent with the sub-ambient cooling observed in our outdoor experiment. However, this strategy becomes more challenging at locations closer to the equator. For example, in Marrakesh, Morocco, the maximum solar elevation angle can reach around 82°, meaning that the sun is nearly overhead during part of the day. In such cases, a fixed vertical sun shield may only work during periods with lower solar elevation angles or would require a much larger shield. Therefore, improved shielding designs, such as solar-tracking shields or elevated partial shields placed above the radiative cooler [34], may be needed for all-day operation in low-latitude regions.

Table 3 summarizes representative PDMS-based radiative cooling studies and the substrate types used in each work. Compared with previous studies that focused on specific PDMS structures or mainly laboratory-prepared reflective substrates, the present work compares flat PDMS films on both transparent silica and a commercial sunlight reflector over a broad thickness range.

4. Conclusion

In this study, we conducted a systematic investigation of the optical and radiative cooling performance of PDMS based passive daytime radiative cooling materials on both high transparent and high reflective substrates. PDMS films with thicknesses ranging from around 1 μm to around 1000 μm were fabricated on fused silica wafers and commercial sunlight reflector substrates, and their optical properties were measured across the solar and mid infrared spectrum. The numerical cooling model was then used to quantify the cooling power of each configuration.

For the high transparent PDMS based PDRC materials, the results show that all PDMS thicknesses from 1.7 μm to 121 μm exhibit high solar transmittance and strong mid infrared emissivity, leading to similar cooling performance with a relative difference of less than 3%. The numerical model predicts a minimum temperature reduction of approximately 8–9 °C below ambient under the defined simulation conditions. Although thicker PDMS films exhibit higher emissivity, they also experience increased solar absorption, which limits the cooling performance. The analysis indicates that PDMS thicknesses above approximately 60 μm no longer provide additional benefits in emissivity, and coatings below 121 μm are sufficient for practical applications. These findings make thin PDMS layers on transparent substrates highly suitable for hybrid solar utilization where both cooling and solar transmission are desired.

For the high reflective PDMS based PDRC materials, the presence of the sunlight reflector significantly increases solar absorption due to both the intrinsic absorption of silver and the enhanced optical path length created by multiple reflections within the PDMS layer. Although increasing the PDMS thickness improves mid infrared emissivity, the associated increase in solar absorption ultimately limits the achievable cooling power. The optimal PDMS thickness for the reflective configuration is approximately 60 μm, but even this configuration does not provide strong sub ambient cooling under direct sunlight. These results demonstrate that unmodified commercial sunlight reflectors present challenges for daytime radiative cooling unless additional optical strategies are employed.

Composite structures or porous coatings may improve the mechanical robustness of polymer-based PDRC materials for applications such as rooftops, façades, and outdoor devices. However, their optical properties must be carefully evaluated, as fillers or structural changes may affect solar absorptance and mid-infrared emissivity.

Although PDMS-based PDRC materials show promising optical and radiative cooling performance, their practical outdoor application still requires further consideration of long-term durability, mechanical robustness, surface contamination, and environmental stability. Future work should therefore evaluate these factors while ensuring that the low solar absorptance and high mid-infrared emissivity required for radiative cooling are maintained.

Overall, this work provides a comprehensive database of the optical and cooling characteristics of simple, flat PDMS films on transparent and reflective substrates. These results offer clear guidance for designing PDMS based radiative cooling materials and identifying optimal

Table 3
Comparison of representative PDMS-based radiative cooling studies with the present work.

Ref.	Material/structure	Substrate type	Main fabrication route	Main focus	Key difference from the present work
Huang et al., 2024 [14]	Transparent polymer-based metamaterial with PDMS microstructures	Soda-lime glass	Micro-structuring and polymer-based metamaterial fabrication	Transparent radiative cooling, indoor light management, and self-cleaning	Focuses on structured multifunctional transparent metamaterials for radiative cooling, indoor light management, and self-cleaning
Zhou et al., 2019 [15]	PDMS-coated metal-reflector structure	Aluminium foil reflector	Solution coating of PDMS on metal	All-day radiative cooling using PDMS-coated metal-reflector structures	Demonstrates PDMS/metal reflector cooling performance
Zhou et al., 2021 [16]	Porous PDMS sponge	No reflector substrate	Casting	Low-cost porous PDMS radiative cooling	Uses porous PDMS to enhance solar scattering and thermal emission
Herrmann et al., 2022 [17]	Homogeneous PDMS films	Silver-coated silica reflector substrate	Flat PDMS film coating on silver reflector	PDMS thickness optimization	Focuses on silver reflector-backed PDMS films
Kou et al., 2017 [18]	Homogeneous PDMS films	Silver-coated silica reflector substrate	Polymer coating on reflective mirror structure	Simple polymer-based daytime radiative cooling	Focuses on silver reflector-backed PDMS films
Present work	Flat PDMS films	Transparent fused silica substrate and commercial sunlight reflector	Spin coating, blade coating, and mould casting	Thickness-dependent optical properties and cooling performance	Compares transparent and reflective PDMS-based PDRC configurations; uses commercial solar reflector

thickness ranges for different application scenarios.

Long-term outdoor stability is another important factor for practical applications of PDMS-based PDRC materials. Compared with many common polymers, PDMS shows relatively good outdoor robustness due to its chemical stability, UV resistance, and thermal stability [35,36]. Its hydrophobic surface can also help reduce water retention and provide a certain self-cleaning effect under rain. However, dust accumulation, surface contamination, rain erosion, and long-term weathering may still gradually change the solar transmittance/reflectance and mid-infrared emissivity, thereby affecting cooling performance. Further efforts are therefore needed to enhance the outdoor durability of PDMS-based PDRC materials, for example by introducing lotus-leaf-inspired microstructures or other self-cleaning surface designs [14], while ensuring that the required low solar absorption and high mid-infrared emissivity are maintained.

Author contributions

G.H. developed the concept and research methodology. Z.S. (lead), P. P., H.C. and G.H. fabricated the samples, conducted the experiment and simulation. Z.S., G.H. and B.S.R. conducted analysis of the research results. Z.S., G.H. and B.S.R. contributed to writing and revising the manuscript. G.H. directed and supervised this project.

Declaration of competing interest

The authors declare no competing interests.

Acknowledgements

The authors gratefully acknowledge financial support received from: i) This work was supported by the Initiative and Networking Fund of the Helmholtz Association under the call Helmholtz Investigator Group (VH-NG-21-07, UNICOS) by G.H. ii) the Helmholtz Association Research Field Energy: Program Materials and Technologies for the Energy Transition (Topic 1 Photovoltaics and Wind Energy, ref. 35.01.04) by B. S.R. and G.H.; iii) the Karlsruhe School of Optics and Photonics (KSOP) by Z.S., B.S.R. and G.H. The authors also wanted to thank Dr. Dmitry Busko for the support in PDMS preparation, Mr. Ivan Alberto Cruz Garcia and Mr. Deep Mandavia for their support in outdoor experiments.

Data availability

The data are available upon reasonable request from the authors.

References

[1] Bin Zhao, Hu Mingke, Xianze Ao, Nuo Chen, Gang Pei, Radiative cooling: a review of fundamentals, materials, applications, and prospects, Appl. Energy 236 (2019) 489–513. ISSN 0306–2619.
[2] S. Fan, W. Li, Photonics and thermodynamics concepts in radiative cooling, Nat. Photonics 16 (2022) 182–190.
[3] J. Liu, Y. Zhang, D. Zhang, S. Jiao, Z. Zhang, Z. Zhou, Model development and performance evaluation of thermoelectric generator with radiative cooling heat sink, Energy Convers. Manag. 216 (2020) 112923, https://doi.org/10.1016/j.enconman.2020.112923.
[4] R.W. Bliss, Atmospheric radiation near the surface of the ground: a summary for engineers, Sol. Energy 5 (3) (1961) 103–120.
[5] M. Chen, D. Pang, X. Chen, H. Yan, Y. Yang, Passive daytime radiative cooling: fundamentals, material designs, and applications, EcoMat 4 (1) (2022) e12153.
[6] L. Liu, J. Wang, Q. Li, Passive daytime radiative cooling polymeric materials: structure design, fabrication, and applications, Appl. Mater. Today 39 (2024) 102331.
[7] R. Liu, et al., Materials in radiative cooling technologies, Adv. Mater. 37 (2) (2025) 2401577.
[8] Sunae So, Jooyeong Yun, Byoungsu Ko, Dasol Lee, Minkyung Kim, Jaebum Noh, Cherry Park, Junkyeong Park, Junsuk Rho, Radiative cooling for energy sustainability: from fundamentals to fabrication methods toward commercialization, Adv. Sci. 11 (2) (2024) 2305067.
[9] Wei Xie, Chengyu Xiao, Ya Sun, Yile Fan, Binyuan Zhao, Di Zhang, Tongxiang Fan, Han Zhou, Flexible photonic radiative cooling films: fundamentals, fabrication and applications, Adv. Funct. Mater. 33 (46) (2023) 2305734.
[10] Minjae Lee, Gwansik Kim, Yeongju Jung, Kyung Rok Pyun, Jinwoo Lee, Byung-Wook Kim, Seung Hwan Ko, Photonic structures in radiative cooling, Light Sci. Appl. 12 (1) (2023) 134.
[11] A.P. Raman, M.A. Anoma, L. Zhu, E. Rephaeli, S. Fan, Passive radiative cooling below ambient air temperature under direct sunlight, Nature 515 (7528) (2014) 540–544.
[12] J. Mandal, Y. Fu, A.C. Overvig, M. Jia, K. Sun, N.N. Shi, Y. Yang, Hierarchically porous polymer coatings for highly efficient passive daytime radiative cooling, Science 362 (6412) (2018) 315–319.
[13] K. Lin, S. Chen, Y. Zeng, T.C. Ho, Y. Zhu, X. Wang, C.Y. Tso, Hierarchically structured passive radiative cooling ceramic with high solar reflectivity, Science 382 (6671) (2023) 691–697.
[14] Gan Huang, Ashok R. Yengannagari, Kishin Matsumori, Prit Patel, Anurag Datla, Karina Trindade, Enkhlen Amarsanaa, et al., Radiative cooling and indoor light management enabled by a transparent and self-cleaning polymer-based metamaterial, Nat. Commun. 15 (1) (2024) 3798.
[15] Lyu Zhou, Haomin Song, Jianwei Liang, Matthew Singer, Ming Zhou, Edgars Stegenburgs, Nan Zhang, et al., A polydimethylsiloxane-coated metal structure for all-day radiative cooling, Nat. Sustainability 2 (8) (2019) 718–724.
[16] Lyu Zhou, Jacob Rada, Huafan Zhang, Haomin Song, Seyededriss Mirniaharikandi, Boon S. Ooi, Qiaoqiang Gan, Sustainable and inexpensive polydimethylsiloxane sponges for daytime radiative cooling, Adv. Sci. 8 (23) (2021) 2102502.
[17] Kai Herrmann, Tobias Lauster, Qimeng Song, Markus Retsch, Homogeneous polymer films for passive daytime cooling: optimized thickness for maximized cooling performance, Adv. Energy Sustainability Res. 3 (2) (2022) 2100166.
[18] J.L. Kou, Z. Jurado, Z. Chen, S. Fan, A.J. Minnich, Daytime radiative cooling using near-black infrared emitters, ACS Photonics 4 (3) (2017) 626–630.
[19] P. Ghosh, X. Wei, H. Liu, Z. Zhang, L. Zhu, Simultaneous subambient daytime radiative cooling and photovoltaic power generation from the same area, Cell Rep. Phys. Sci. 5 (3) (2024).
[20] G. Huang, E. Gage, B. Breiner, M. Saavedra, D. Busko, N.J. Janowicz, B.S. Richards, Broad-range spectral management towards next-generation net-zero energy greenhouses, Energy Environ. Sci. 18 (21) (2025) 9435–9445.
[21] K. Lin, et al., A flexible and scalable solution for daytime passive radiative cooling using polymer sheets, Energ. Buildings 252 (2021) 111400.
[22] C.A.R. Mazelin, A Brief Review of Sylgard 184, Los Alamos National Laboratory (LANL), Los Alamos, NM (United States), 2023. LA-UR-23-22758.
[23] Z. Brounstein, J. Zhao, D. Geller, N. Gupta, A. Labouriau, Long-term thermal aging of modified Sylgard 184 formulations, Polymers (Basel) 13 (18) (2021) 3125.
[24] Alanod, MIRO® High Reflective 95.
[25] Md.M. Hossain, M. Gu, Radiative cooling: principles, progress, and potentials, Adv. Sci. 3 (7) (2016) 1500360.
[26] E. Rephaeli, A. Raman, S. Fan, Ultrabroadband photonic structures to achieve high-performance daytime radiative cooling, Nano Lett. 13 (4) (2013) 1457–1461.
[27] X. Yu, J. Chan, C. Chen, Review of radiative cooling materials: performance evaluation and design approaches, Nano Energy 88 (2021) 106259.
[28] M.P. Wolf, G.B. Salieb-Beugelaar, P. Hunziker, PDMS with designer functionalities—properties, modifications strategies, and applications, Prog. Polym. Sci. 83 (2018) 97–134.
[29] A. Victor, J.E. Ribeiro, F.F. Araújo, Study of PDMS Characterization and its Applications in Biomedicine: A Review, 2019.
[30] S. Katz, et al., Studying the physical and chemical properties of polydimethylsiloxane matrix reinforced by nanostructured TiO2 supported on mesoporous silica, Polymers 15 (1) (2022) 81.
[31] M.J. Chowdhury, J. Lou, D. Kuila, D. Mukherjee, Polydimethylsiloxane based mixed matrix membranes with pretreated fumed silica for efficient CO2 separation, Sci. Rep. 15 (1) (2025) 36401.
[32] R.P.C.L. Sousa, B. Ferreira, M. Azenha, S.P.G. Costa, C.J.R. Silva, R.B. Figueira, PDMS based hybrid sol-gel materials for sensing applications in alkaline environments: synthesis and characterization, Polymers 12 (2) (2020) 371.
[33] V.-M. Graubner, et al., Photochemical modification of cross-linked poly (dimethylsiloxane) by irradiation at 172 nm, Macromolecules 37 (16) (2004) 5936–5943.
[34] B. Bhatia, A. Leroy, Y. Shen, L. Zhao, M. Gianello, D. Li, E.N. Wang, Passive directional sub-ambient daytime radiative cooling, Nat. Commun. 9 (1) (2018) 5001.
[35] K.R. McIntosh, N.E. Powell, A.W. Norris, J.N. Cotsell, B.M. Ketola, The effect of damp-heat and UV aging tests on the optical properties of silicone and EVA encapsulants, Prog. Photovolt. Res. Appl. 19 (3) (2011) 294–300.
[36] Y. Xiu, L. Zhu, D. Hess, C.P. Wong, Superhydrophobicity and UV stability of polydimethylsiloxane/polytetrafluoroethylene (PDMS/PTFE) coatings, in: 2006 11th International Symposium on Advanced Packaging Materials: Processes, Properties and Interface, IEEE, 2006, pp. 98–103.